Article

High-frequency surface acoustic wave device based on thin-film piezoelectric interdigital transducers

SARIN KUMAR, Koyilothu, *et al*.

High-frequency surface acoustic wave device based on thin-film piezoelectric interdigital transducers

A. K. Sarin Kumar,[a] P. Paruch, and J.-M. Triscone[b]
DPMC, University of Geneva, 24 Quai E. Ansermet, 1211 Geneva 4, Switzerland

W. Daniau and S. Ballandras
Laboratoire de Physique et Métrologie des Oscillateurs, CNRS UPR3203, 32 Avenue de l'Observatoire, F25044, Besançon, France

L. Pellegrino and D. Marré
INFM, Research unit of Genoa, Dodecaneso 33, 16146 Genova, Italy

T. Tybell
Department of Electronics and Telecommunications, Norwegian University of Science and Technology, 7491 Trondheim, Norway

(Received 21 April 2004; accepted 9 July 2004)

Using high-quality epitaxial *c*-axis $Pb(Zr_{0.2}Ti_{0.8})O_3$ films grown by off-axis magnetron sputtering onto metallic (001) Nb-doped $SrTiO_3$ substrates, a nonconventional thin-film surface acoustic wave device based on periodic piezoelectric transducers was realized. The piezoelectric transducers consist of a series of ferroelectric domains with alternating polarization states. The artificial modification of the ferroelectric domain structure is performed by using an atomic force microscope tip as a source of electric field, allowing local switching of the polarization. Devices with 1.2 and 0.8 μm wavelength, defined by the modulation period of the polarization, and corresponding to central frequencies in the range 1.50–3.50 GHz have been realized and tested. © *2004 American Institute of Physics*. [DOI: 10.1063/1.1787897]

Surface acoustic waves (SAW) are used for filtering applications in mobile communication and for passive signal processing devices, such as delay lines and resonators.[1] It is expected that the frequency range allocated for personal media communications will increase into the 5–10 GHz range,[2] requiring high-frequency SAW filters.[3] High-frequency SAW devices would not only be useful in future applications, but could also be of interest in the study of liquid-solid interfaces, or electron-phonon interactions.[4–7]

In classical SAW devices, periodic metallic interdigital transducers (IDTs), deposited on uniformly polarized piezoelectric crystals or films, act as electric input and output ports.[8] The application of an appropriate radio frequency (rf) signal to the IDT produces a deformation of the material surface and results in the launching of SAW, which travel along the piezoelectric surface with a phase velocity given by the physical properties of the material. These surface waves can then be converted back to an electric signal by a receiving IDT. The center frequency (f_c) of the SAW device is given by $f_c = v_p/\lambda$, where the wavelength λ is the distance between the IDT fingers of the same electrode, and v_p is the phase velocity in the material. In order to increase f_c, either the wavelength of the device has to be decreased or a material with a higher phase velocity has to be used as the traveling medium. Typical phase velocities of most piezoelectric materials are between 2500–6000 m/s resulting in working frequencies of 1–3 GHz when standard photolithography (minimum finger width 0.5 μm) is used for defining the IDTs. Prototype SAW filters in the GHz range have also been demonstrated by growing the piezoelectric materials on substrates with high phase velocities like diamond or sapphire.[9–11] Another approach to reaching higher working frequencies is to fabricate devices with smaller wavelengths by decreasing the distance between the IDT fingers, for instance by using electron beam lithography. With this technique, prototype devices with wavelengths smaller than 1 μm have been fabricated, leading to center frequencies of up to 20 GHz.[11,12]

In this letter we report on the modeling, fabrication, and electrical measurements of prototype SAW devices based on a nonconventional transducer principle. We show that nanoscale ferroelectric domain manipulation and atomic force microscopy (AFM) writing of periodic piezoelectric transducers in epitaxial films is a promising approach, allowing the implementation of very high-frequency SAW devices.

In this original device, the conventional metallic IDT has been replaced by a piezoelectric interdigital transducer (PIT) consisting of oppositely polarized ferroelectric domains, schematically illustrated in Fig. 1(a). Such a transducer is fabricated by writing line-shaped domains with alternating polarization on high-quality *c*-axis $Pb(Zr_{0.2}Ti_{0.8})O_3$ (PZT) films grown on metallic (001) Nb:$SrTiO_3$ substrates.[13] The local polarization control is achieved by using the metallic tip of an AFM as a local electric-field source, applying a voltage between the tip and the conducting substrate (used as the ground electrode).[14,15] In previous studies on similar films, it was shown that domains with radii as small as 20 nm can be written down to 10 nm apart using AFM.[15] This control directly determines the precision at which the PIT can be written and the minimum wavelength of the device. To excite the PIT, a single electrode is deposited on its surface [see Fig. 1(a)], in contrast to standard SAW devices, and a rf voltage is then applied between the top electrode and the conducting substrate. Since the sign of the piezoelectric coefficient depends on the polarization direction, the applied rf

[a]Present address: Department of Electonics and Telecommunications, Norwegian University of Science and Technology,7491 Trondheim, Norway.
[b]Author to whom correspondence should be addressed; electronic mail: Jean-Marc.Triscone@Physics.UniGE.ch

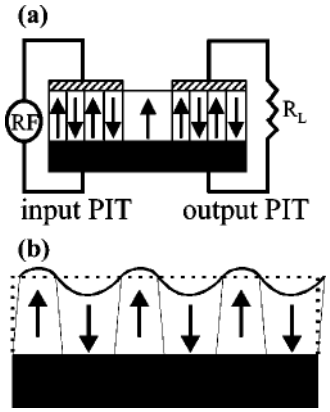

FIG. 1. A schematic diagram of the SAW device with PITs (piezoelectric IDTs). The PITs are made of ferroelectric domains with alternating polarization states written in the *c*-axis oriented PZT films. (b) Schematic representation of the domain deformation with applied rf voltage. The deformation (elongation or contraction) for a given voltage depends on the polarization direction.

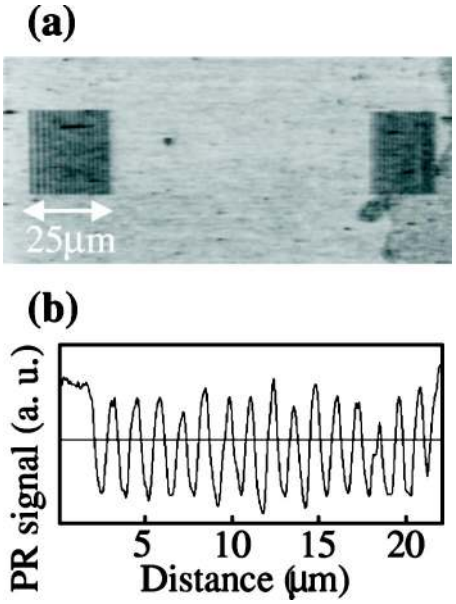

FIG. 2. Piezoelectric microscopy image of one of the prototype SAW devices.The distance between the input and output PIT is around 70 μm and that between two adjacent line-shaped domains of opposite polarization is 0.6 μm, leading to a 1.2 μm wavelength. (b) Line section through piezoresponse (PR) image of one of the PITs.

voltage will produce a deformation (elongation or contraction) of the domains, as shown in Fig. 1(b), launching a surface wave when $\lambda f_c = v_p$. This mechanical deformation of the material is complex, with one end of the domains being "clamped" to the substrate, which is assumed to be rigid and the other end being essentially free to deform (although covered by the electrode). The wavelength λ of the device is the distance between the domains of the same polarization, contrary to standard IDT-based SAW devices for which the wavelength equals twice the mechanical period of the gratings. Consequently, for any given resolution, the operating frequency of PIT-based SAW devices is expected to be twice that of a standard SAW device. Furthermore, the size of the domains can be controlled by AFM and thus made very small. These are the main innovations of the proposed approach, which can lead to the fabrication of very high-frequency SAW filters, possibly above 20 GHz.

To further understand the behavior of such a structure, numerical simulations have been performed.[16] In these simulations, the elementary cell of the periodic array is composed of a 0.2-μm-thick $PbZr_{0.5}Ti_{0.5}O_3$ layer deposited on a (001) $SrTiO_3$ substrate (considered electrically conductive) with a Pt electrode above the piezoelectric layer. The polarization is assumed to exhibit a 1.2 μm period, which is the wavelength of one of the devices described below. The harmonic admittance is then computed assuming an infinite periodic structure excited in phase. Four coupled modes are found at 1.57 GHz ($v_p = 1884$ m/s, $K_s^2 = 14.5\%$), 2.02 GHz ($v_p = 2424$ m/s, $K_s^2 = 2.4\%$), 2.96 GHz ($v_p = 3552$ m/s, $K_s^2 = 1.8\%$) and 3.90 GHz ($v_p = 4680$ m/s, $K_s^2 = 7.2\%$), where K_s^2 is the electromechanical coupling coefficient. An interesting result of the simulation is that the wave radiation losses into bulk started appearing only around 4 GHz, in contrast to conventional devices where bulk radiation occurs around 2 GHz. This suggests that bulk acoustic energy radiation loss is reduced in this transducer geometry as compared to conventional SAW devices.

To experimentally test the PIT principle, *c*-axis-oriented epitaxial PZT films ~0.2 μm thick were fabricated on (001) Nb:$SrTiO_3$ (0.2 at. wt. % Nb) by off-axis rf magnetron sputtering. The details of the preparation and characterization can be found in Ref. 17. X-ray diffraction analysis reveals only *c*-axis reflections with FWHM (full width at half maximum) values of 0.05 and 0.15° for the (001) and (002) peaks, respectively. Topographic measurements of the sample surfaces using AFM revealed smooth surfaces with a root-mean-square roughness of typically 3 Å. To fabricate the PITs, a 150×100 μm^2 area was first defined photolithographically on the film.[18] An area of around 130×65 μm^2 was then uniformly polarized by slowly scanning the AFM tip while applying a constant −12 V between the tip and the conducting substrate. This prepoling is performed to avoid any domain-wall scattering of the surface waves traveling between the PITs. The input and output PITs were then fabricated by writing line-shaped domains with alternating polarization inside a 20×20 μm^2 area by alternately applying a + and −12 V bias to the tip. The accuracy of the domain width is typically ±0.08–0.1 μm. Subsequently, Pt electrodes with a thickness of 20 nm were sputtered on the PITs. Figure 2(a) shows a piezoelectric microscopy image of a prototype SAW device. Here, the distance between the input and output PITs is around 70 μm and that between two adjacent line-shaped domains of opposite polarization is 0.6 μm, leading to a wavelength of 1.2 μm. Figure 2(b) shows a line section through the piezoresponse image of one of the PITs. It is interesting to note that the size of this SAW device is typically 100×100 μm^2. Based on ladder architecture, one can expect further size reduction using PIT-based structures in comparison with standard IDT-based devices for similar wavelengths.[9]

One of the critical issues regarding this device is the stability of the written ferroelectric domains. Heat treatment (during photolithographic processes) and the applied electric field during device operation could lead to instabilities of the artificially written domain structure. For the former case it has been found that the domains are stable for more than three months (the duration of the measurements), even after heating to 250°C and heavy photolithographic processing. To estimate the effect of the electric field on domain-wall

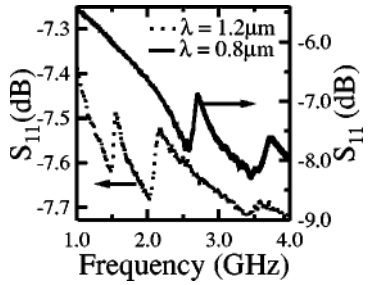

FIG. 3. Reflection (S_{11}) spectra of 1.2 μm (dotted line) and 0.8 μm (solid line) wavelength devices with PITs.

motion, we calculated the maximum field applied to the device (about 2×10^4 V/cm, below the 10^5 V/cm PZT coercive field) to get the domain-wall velocity.[19] A velocity of about $\sim10^{-11}$ m/s was found, leading to negligible domain-wall motion for the high working frequencies used here.

Electrical measurements were carried out using an Anritsu ® network analyzer and a set of Picoprobe ® coplanar probes.[20] Since our substrate is metallic and also partly because of the high PZT losses, a significant damping of the SAW is observed in this prototype device, not allowing direct SAW transmission measurements to be performed. For this reason, we focus here on the S_{11} reflection measurements which allow us to demonstrate the PIT-operation. Figure 3 shows the reflection measurement (S_{11}) results of the PIT-based SAW devices with different wavelength in the frequency range of 3 GHz. For a 1.2 μm device (dotted line), two reflection minima at 1.50 and 2.02 GHz are observed, in good agreement with the first two modes (1.57 and 2.02 GHz) observed in the simulation results described above. In a first-order approximation (i.e., neglecting the dispersion behavior), a change in wavelength will produce a corresponding change in the working frequency of the device. For example, a wavelength change from 1.2 to 0.8 μm would correspond to a frequency shift of 1.5. To test this, we fabricated another device with a wavelength of 0.8 μm. The result for the 0.8 μm device is shown in Fig. 3 (solid line). Two reflection minima close to 2.57 and 3.44 GHz can be seen, corresponding to a frequency shift of 1.7 with respect to the 1.2 μm device. This small discrepancy in frequency ratio from the expected value of 1.5 is not unreasonable in a first-order approximation, and taking into account the writing errors in the linewidth of each domain, $\pm0.08-0.1$ μm. These results are an experimental demonstration related to the launching of a SAW using PITs.

With the above mentioned experimental observations, one can conclude that the PITs operate in accordance with the basic SAW equation, $f_c=v_p/\lambda$, and in agreement with the simulations. According to theoretical analysis, the reflection minima observed experimentally in the vicinity of 2.02 GHz ($\lambda=1.2$ μm) and 3.44 GHz ($\lambda=0.8$ μm) will correspond to the vibration mode shown in Fig.1(b). However, the contribution close to 1.5 GHz ($\lambda=1.2$ μm) and 2.57 GHz ($\lambda=0.8$ μm) is less intuitive and is the equivalent of an antisymmetric Lamb mode of the PZT layer. A small contribution is also observed at 3.4 GHz ($\lambda=1.2$ μm), for which a match with the simulation is more difficult to establish. The reflection curves reported in Fig. 3 also show damped contributions, whereas sharper peaks are expected from theoretical analyses, which include only losses due to acoustic radiation in the substrate. This suggests that other sources of losses have to be considered in the computations. For instance, PZT has performed poorly in rf applications[21–23] and may thus be a source of important losses. Also, conduction currents due to the wave penetration may be generated in the substrate yielding additional losses.[24] More experimental studies are in progress to address these issues.

In conclusion, we have proposed an original transducer concept for rf SAW devices based on a periodic distribution of oppositely poled piezoelectric domains and succeeded in fabricating prototypes of such devices on epitaxial PZT films prepared on metallic Nb-$SrTiO_3$ substrates. The measured S_{11} parameter for the two devices with different wavelengths exhibited a clear shift in frequency response in agreement with the basic principle of SAW devices.

This work was supported by the Swiss National Science Foundation through the National Centre of Competence in Research "Materials with Novel Electronic Properties-MaNEP" and Division II, NEDO, and ESF (Thiox).

[1] C. C. W. Ruppel, R. Dill, A. Fischerauer, G. Fischerauer, W. Gawlik, J. Machui, F. Muller, L. Reindl, W. Ruile, G. Scholl, I. Schropp, and K. Ch. Wagner, IEEE Trans. Ultrason. Ferroelectr. Freq. Control **40**, 438 (1993).
[2] K. M. Larkin, G. R. Kline, and T. McCarron, IEEE Trans. Microwave Theory Tech. **43**, 2933 (1995).
[3] S.-H. Lee, K. H. Yoon, and J.-K. Lee, Appl. Phys. Lett. **92**, 4062 (2002), and references therein.
[4] R. W. Morse and H. V. Bohm, Phys. Rev. **108**, 1094 (1957).
[5] D. J. Bishop, C. M. Varma, B. Batlogg, and E. Bucher, Phys. Rev. Lett. **53**, 1009 (1984).
[6] M. Saint-Paul, F. Pourtier, B. Pannetier, J. C. Villegier, and R. Nava, Physica C **183**, 257 (1991).
[7] S.–G. Lee, C.–C. Chi, G. Koren, and A. Gupta, Phys. Rev. B **43**, 5459 (1991).
[8] R. M. White and F. W. Voltmer, Appl. Phys. Lett. **7**, 314 (1965).
[9] C. K. Campbell, *Surface Acoustic Wave Devices for Mobile and Wireless Communications* (Academic, San Diego, 1998).
[10] H. Nakahata, K. Higaki, A. Hachigo, S. Shikata, N. Fujimori, Y. Takahashi, T. Kajihara, and Y. Yamamoto, Jpn. J. Appl. Phys. **33**, 324 (1994).
[11] Y. Takagaki, P. V. Sanots, E. Wiebicke, O. Brandt, H.-P. Schönherr, and K. H. Ploog, Appl. Phys. Lett. **81**, 2538 (2002).
[12] S. Lehtonen, J. Koskela, M. M. Salomaa, V. P. Plessky, M. Honkanen, and J. Turunen, Appl. Phys. Lett. **75**, 142 (1999).
[13] A. K. Sarin Kumar, P. Paruch, D. Marré, L. Pellegrino, T. Tybell, S. Ballandras, and J.-M. Triscone, Integr. Ferroelectr. **63**, 55–62 (2004); D. Marré, T. Tybell, C. Beneduce, and J.-M. Triscone (to be published).
[14] C. H. Ahn, T. Tybell, L. Antognazza, K. Char, R. H. Hammond, M. R. Beasley, Ø Fisher, and J.-M. Triscone, Science **276**, 1100 (1997).
[15] P. Paruch, T. Tybell, and J.-M. Triscone, Appl. Phys. Lett. **79**, 530 (2001).
[16] S. Ballandras, V. Laude, Th. Pastureaud, M. Wilm, W. Daniau, A. Reinhardt, W. Steichen, and R. Lardat, Proc.-IEEE Ultrason. Symp. **1**, 321 (2002).
[17] T. Tybell, C. H. Ahn, and J.-M. Triscone, Appl. Phys. Lett. **75**, 856 (1999).
[18] Amorphous, 250-nm-thick CeO2 were deposited everywhere on PZT films except in the defined 150×100 μm^2, allowing us to reduce the capacitance of the device.
[19] T. Tybell, P. Paruch, T. Giamarchi, and J.-M. Triscone, Phys. Rev. Lett. **89**, 097601 (2002).
[20] Before the transmission measurements, we calibrated the network analyzer using an impedance standard substrate.
[21] Q.-X. Su, P. Kirby, E. Komuro, M. Imura, Q. Zhang, R. Whatmore, IEEE Trans. Ultrason. Ferroelectr. Freq. Control **49-4**, 769 (2001).
[22] T. Omori, H. Makita, M. Takamatsu, K. Y. Hashimoto, and M. Yamaguchi, Proc.-IEEE Ultrason. Symp. **2**, 995 (1999).
[23] M. Yamaguchi, K. Hashimoto, R. Nanjo, H. Hanazawa, S. Tsutsumi, and T. Yonezawa, Proc. IEEE-IFCS Frequency Control Symposium, **1**, 544 (1997).
[24] M. Solal, Th. Pastureaud, S. Ballandras, B. Aspar, B. Biasse, W. Daniau, J. M. Hode, S. Calisti, and V. Laude, Proc.-IEEE Ultrason. Symp. **1**, 131 (2002).